CHALMERS
UNIVERSITY OF TECHNOLOGY

Kinetic modelling of gas-phase reactions of polyethylene-derived pyrolysis products in steam gasification

Master's thesis in Master Programme Sustainable Energy Systems

HANNA BENGTSSON

Department of Space, Earth and Environment
CHALMERS UNIVERSITY OF TECHNOLOGY
Gothenburg, Sweden 2018

Master's thesis

Kinetic modelling of gas-phase reactions of polyethylene-derived pyrolysis products in steam gasification

HANNA BENGTSSON

CHALMERS
UNIVERSITY OF TECHNOLOGY

Department of Space, Earth and Environment
Division of Energy Technology
Chalmers University of Technology
Gothenburg, Sweden 2018

Kinetic modelling of gas-phase reactions of polyethylene-derived pyrolysis products in steam gasification
HANNA BENGTSSON

Supervisor: Teresa Berdugo Vilches & Huong Nguyen, Department of Space, Earth and Environment
Examiner: Martin Seemann, Department of Space, Earth and Environment

Master's Thesis
Department of Space, Earth and Environment
Division of Energy Technology
Chalmers University of Technology
SE-412 96 Gothenburg
Telephone +46 31 772 1000

Gothenburg, Sweden 2018

Kinetic modelling of gas-phase reactions of polyethylene-derived pyrolysis products in steam gasification

HANNA BENGTSSON

Division of Energy Technology
Department of Space, Earth and Environment
Chalmers University of Technology

Abstract

Today, only 15% of the plastic waste in Europe is recycled. However, the existing recycling processes used, cannot preserve the quality of the material. The main production of plastic products is based on fossil resources and to ensure future assets, and to reduced environmental impact, new technology for recycling is demanded. Gasification of plastic has so far been utilized for production of fuels, and the next step is the possibility of production of hydrocarbon monomers.

Gasification of hydrocarbon polymers includes an initial step of pyrolysis, followed by secondary gas-phase reactions of the volatile pyrolysis products and the gasifying agent. In this Master's Thesis, a kinetic model of the secondary gas-phase reactions of polyethylene steam gasification at 700-800°C, is formulated. Based on existing hydrocarbon thermodynamic and kinetic mechanisms, a plug flow model is simulated in ANSYS Chemkin-Pro, with an input of polyethylene-derived pyrolysis products obtained from earlier published literature. From the simulated results it is concluded, that the provided input temperature profiles and sets of reactant input compositions, have low influence on the obtained results. Instead, the residence time shows the highest influence of the progress of product specie concentrations, where the largest increase occurs within 20 ms. Study of reaction pathways for the applied conditions, show that in relation to ethylene, the simulated results are similar to literature of pyrolysis and combustion processes. In relation to existing experimental data of polyethylene steam gasification, from the gasification unit in Chalmers Power Central, the simulated yields are overall higher for the hydrocarbon species, while the products of the water-gas shift reaction are underestimated.

The formulated model can further be used for explicit examination of specific mechanisms related to the process of steam gasification of hydrocarbon polymers. The model set-up provides the possibility to study different conditions regarding temperature, pressure, residence time and reactant input composition.

Keywords: fluidized bed, kinetic simulation, plastic waste, polyethylene, pyrolysis, reaction network, secondary gas-phase reaction, steam gasification.

Acknowledgements

The subject of plastic waste afterlife has been topical in the media during the winter and spring of 2018. Also, the European Comission recently decided on new targets for plastic recycling, demanding new ways of material recycling to ensure a more sustainable environmental and socioeconomic future, which brings us to the topic of this Master's Thesis. The work of this project has been both interesting, challenging and fun. First of all, I want to express my gratitude to my supervisors Huong Nguyen and Teresa Berdugo Vilches, for the guidance and feedback you have provided for me during this project. Thanks for interesting discussions, which have challenge me and improved my academic development.

Further, I would like to thank Martin Seeman for providing me the opportunity to work on this project. The topic of polymer gasification presents an interesting option of recycling of plastic materials, in order to save resources and improve circular economy. It is clear that there is still a lot to discover within this field, and it will be exiting to follow the progress in the future.

I also want to thank the "gasification group" at the department, for including me within your monthly meetings and for the opportunity to come along to the Swedish Gasification Centre (SFC) conference in February. Last but not least, a big thanks to Niklas, my family and friends, for all your encouragement and support during my time at Chalmers, and especially during these last months.

Hanna Bengtsson, Gothenburg, June 2018

Contents

List of Figures

List of Tables

List of Abbreviations

Abbreviations

daf ..... dry ash-free

GC ..... Gas chromatography

HACA ..... Hydrogen-abstraction acetylene-addition

HDPE ..... High-density polyethylene

LDPE ..... Low-density polyethylene

LLDPE ..... Linear low-density polyethylene

MSW ..... Municipal Solid Waste

PAH ..... Polycyclic Aromatic Hydrocarbons

PE ..... Polyethylene

PFR ..... Plug-flow Reactor

ROP ..... Rate of Production

RPA ..... Reaction Path Analyzer

SPA ..... Solid-Phase Adsorption

Tars ..... Aromatic compounds

WGS ..... Water-gas shift

Symbols

$°C$ ..... degree Celcius

$\dot{m}_{daf}$ ..... mass flow of dry, ash-free fuel $[kg_{daf}\ s^{-1}]$

A ..... area $[m^2]$

C_i ..... concentration $[mol\ {m^3_{wet}}^{-1}]$

E_a ..... activation energy

k ..... kinetic rate constant

kPa ..... kilo pascal

m_i ..... mass $[gram\ {kg_{daf}}^{-1}]$

$M_{w,i}$ ..... molar weight $[g\ mol^{-1}]$

mm ..... millimeters

$mol - \%$ ..... molar precent

ms^{-1} ..... milliseconds

n_i ..... moles $[mol\ kg_{daf}{}^{-1}]$

T ..... temperature

u ..... velocity $[m\ s^{-1}]$

$wt - \%$ ..... mass precent

1. Introduction

Plastic products are used in modern everyday life. A larger share as disposable products which are only used once e.g. plastic bags. Fossil resources are today the primary raw material utilized in the production of plastic polymers. Hydrocarbon monomers are polymerized to chains and, by chemical and/or thermal treatment, plastic materials with different properties are produced. The resistance to degradation is highly efficient during usage. However, as the lifetime of the products is short, the resilience causes problems when plastic waste is deposited in landfills, where it will accumulate or spread to nature causing environmental problems at both land and sea [1, 2]. Other alternatives to landfill is recycling of the material or energy recovery.

1.1 Background

The production rate of plastics in the world has reached over 300 billion tonnes per year and almost 26 billion tonnes of plastic waste is generated in Europe every year. Only a small portion, according to Onwudili et al. (2009) in Europe about 15%, is recycled which results in extensive economic and resource losses [3, 4]. Incineration of plastic waste generates useful energy. However, the process demands comprehensive cleaning of flue gases and carbon dioxide from fossil resources is released to the atmosphere, which makes energy recovery a less efficient and less sustainable choice than recycling [2]. During recycling of plastics, with existing technology, the material is somewhat degraded (i.e. cascade recycling) and cannot produce products of the same quality as the previous. Even though the process of recycling can be more efficient than incineration, the polymers will eventually end up in landfills.

For a sustainable environmental and socioeconomic future the use of resources must be more efficient to avoid depletion and to ensure future assets. Alternatives of bio-based raw materials are at the moment too expensive compared to the production of plastics from fossil-based materials [3], and the today existing options for plastic waste afterlife are not meeting the demand set by the European Commission [2, 4]. Gasification of polymers represents an interesting option of recycling. The material is heated up and initially degraded in an oxygen lean environment, i.e. pyrolysis, before further conversion in the presence of a gasifying agent, e.g. air or steam, occurs. The desired outcome is to obtain monomers, which can be converted into new polymers. The plastic waste is "upgraded" to raw material and retained for future subsequent usage.

As of today, gasification of plastics is mainly utilized for production of fuels, i.e. energy recovery, a process that does not make use of the initial effort that was put into creating the monomers [3].

Research of products from pyrolysis and gasification, of different pure polymer materials and mixtures of polymers, has been performed [5–7]. However, to obtain desired and valuable products, understanding of the process is of great importance. In this work, the reaction steps of steam gasification are examined for a model polymer, polyethylene (PE). Approximately 40% of the plastic content in Western European municipal solid waste (MSW) consists of PE plastics, which makes it an interesting choice of model polymer [6].

1.2 Aim of the thesis

This thesis aims to gain understanding of the process steps and reaction network of hydrocarbon polymer gasification, by formulating a model of the secondary gas-phase reactions of polyethylene-derived pyrolysis products during steam gasification. Knowledge of the gasification process are of importance for design of industrial scale operational conditions, in order to optimize and ensure the desired product outcome, and to maintain as high efficiency as possible during the process.

In the thesis, the process of gasification of PE at an atmospheric pressure and a temperature range of 700-800°C is to be described through kinetic modelling. The mechanisms of gasification of solid PE to product gas, are to be studied and discussed in relation to experimental data obtained at Chalmers Power Central. The work tasks have consisted of: literature study of the process of hydrocarbon pyrolysis; setting up, testing and evaluating a model based on existing kinetic mechanisms; and finally discuss the results in relation to existing experimental data of gasification of PE from Chalmers Power Central. The high temperatures of the gasification unit in the Chalmers Power Central, well above that of PE melting and degradation temperature (500°C) [8], allows for flash pyrolysis, i.e. thermal degradation at high temperature and short residence time, to occur. The primary pyrolysis of PE, from solid granules to gas-phase, is studied in literature where a prescribed gas-phase composition is obtained. Focus of this work is the reactions of the volatile species, where the reaction pathways related to ethylene, benzene and naphthalene are studied in detail.

2. Theory

Polyethylene is a homo-polymer which consists of polymerized ethylene monomers $(C_2H_4)_n$. Depending on the branching of the polymer, different kinds of PE can be produced. Some of the most common kinds are high-density (HDPE), linear low- or low-density PE (LLDPE respectively LDPE). The polymer structure of the three kinds of PE with different densities are presented in Figure 2.1. Variation of the density gives the material different characteristics and makes it usable for a wide range of applications, from soft plastic bags to drainpipes and electric insulation. Common for all PE polymers is that they belong to the family of thermoplastics, meaning that the polymers are connected by intermolecular bonds forming a material that is solid and hard at low temperatures while softening when the temperature is increased [6]. The solid PE melts at a temperature range of 100-140°C, depending on the density, and by further increasing the temperature, the polymer starts to degrade [9].

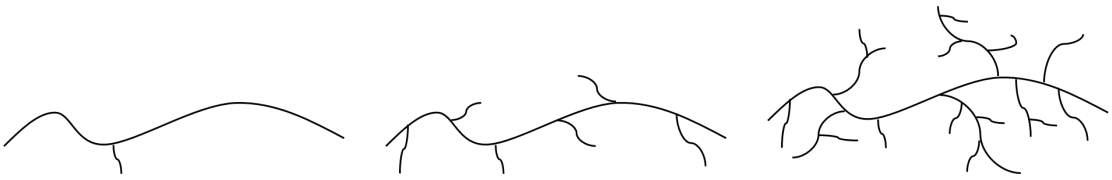

a) High-density b) Linear low-density c) Low-density

Figure 2.1: Polymer structure of three different kinds of polyethylene density, i.e. level of branching.

2.1 Pyrolysis of Polyethylene

The gradual pyrolysis of PE is often described in several steps and in the literature different reaction paths of the pyrolysis have been discussed. According to Westerhout et al., initially primary pyrolysis takes place where the polymer starts to degrade into wax-like materials (Scheme A, Figure 2.2), whereas Onwudili et al. also suggests that direct devolatilization of the polymer occurs, generating gaseous compounds (Scheme B Figure 2.3) [5, 6]. The gas consists mainly of light hydrocarbon species, that are non-condensable at room temperature. Hydrocarbon chains with higher carbon numbers (>C20) forms waxes and denotes the first condensable compounds obtained during the pyrolysis [10].

Further, the waxes will devolatilize into smaller gaseous compounds of paraffins and olefins, example of molecular structure is presented in Figure 2.4a and 2.4b.

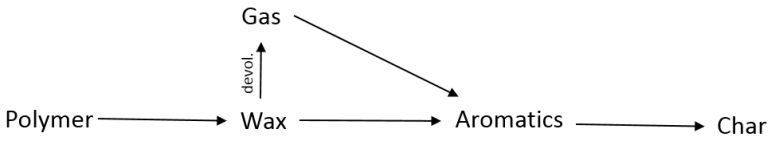

Figure 2.2: Scheme A of polymer pyrolysis with primary conversion to wax. Further, degradation and secondary gas-phase reactions forms light hydrocarbon and aromatic compounds before char formation takes place [5].

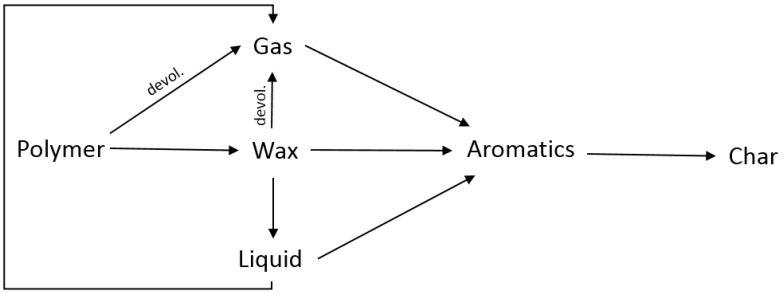

Figure 2.3: Scheme B of polymer pyrolysis with primary conversion to both gaseous and wax compounds. The secondary gas-phase reactions include formation of both light hydrocarbon and aromatic compounds, as well as evaporation and condensation [6].

At high temperatures, the small gaseous olefins and paraffins are unstable and will continue to react with each other, and possibly a gasifying agent. This is called the secondary gas-phase reactions, where both light hydrocarbon species and aromatic compounds (Figure 2.4c) are formed [5]. Onwudili et al. proposes possible additional reaction paths in Figure 2.3, where also a liquid phase is present in the mechanism. For sufficient residence time and temperature, the polymer is converted into char in both schemes [5, 6].

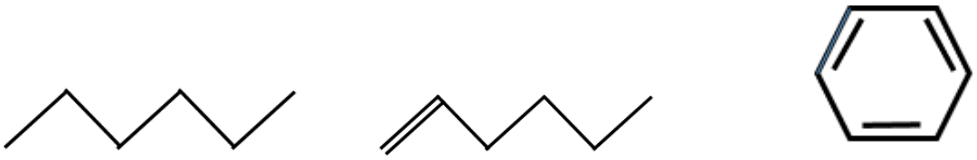

a) Paraffin; Hexane C_6H_{14} b) Olefin; Hexene C_6H_{12} c) Aromatic; Benzene C_6H_6

Figure 2.4: Molecular structure of paraffin, olefin and aromatic.

The final product composition depends on the operational conditions, such are residence time, temperature and gasifying agent. The density of PE has, according to Westerhout et al. (1998) "no significant influence of the product spectrum obtained in pyrolysis", however mixing of PE with different other polymers, e.g. polystyrene or polypropylene, will have an affect on the final product composition [7].

2.1.1 Scissioning of hydrocarbon chain

In 1977, Seeger and Gritter conducted experiments of flash pyrolysis at 780°C with PE and n-paraffins. From these, it was possible to establish a theory of a random degradation mechanism during the primary pyrolysis. The results also indicated that the mechanism was similar for both the shorter hydrocarbon chains with carbon numbers 18-40, as for the longer polymer chain. Also, dissociation of carbon bonds at the end of the chain requires more energy compared to the other carbon bonds not holding an end-group [11]. Later on, Murata et al. (2002) determined for a continuous flow reactor with temperature ranges of 350-450°C, that the activation energy needed for the pyrolysis of polymers (PE included), was high enough to conclude that the rate determining step is the chemical reaction, not the transfer of heat or mass.

Further, it was established that the degradation of PE consisted of both the random and end-chain mechanism [12]. The same scissioning mechanisms are also researched by Ueno et al. (2010), where simulations and experiments, based on the work of Seeger and Gritter (1977); of random scissioning products of PE, were performed with the additional consideration of the effect of volatilization rate. The results concluded that at a temperature of 590°C, no continued degradation of the generated scissioning compounds occurred. This, due to the volatilization rate being faster than the decomposition rate, resulting in a wide range of low- to high-carbon numbered scissioning compounds with and without double bonded carbons (paraffins respectively olefins). When the temperature was increased to 800°C, the decomposition rate exceeded that of volatilization, meaning also secondary gas-phase reactions of scissioning compounds occurred. The distribution of scissioning products changed and the already higher fraction of low carbon numbered compounds increased together with the share of olefins. This also agrees with other works of thermal hydrocarbon degradation [13]. The results of the studies by Ueno and Murata agree on that both the random and end-chain scissioning occur simultaneously and the two studies points towards kinetic scheme B in Figure 2.3.

Of the two scissioning mechanisms mentioned, the end-chain scission is the main source of volatile products and its occurrence increases by temperature [12]. The random scissioning of the main chain occurs through different schemes, were the length of the polymer chain is reduced, i.e. the molecular weight is decreased and the number of molecules increases [8, 12]. C-C and C-H scission, are presented by Ueno et al. (2010) as the two primary pathways of scissioning of the PE main chain, and described in detail in Figure 2.5. These scission mechanisms form radicals that will attract and steal hydrogen from the same polymer chain or intermolecularly.

Further, new radicals or unsaturated carbons are created and the scissioning propagates until stable species are produced. Scissioning pathway a) in Figure 2.5, demands larger energy and consequently pathway b) and c) become the predominant ones.

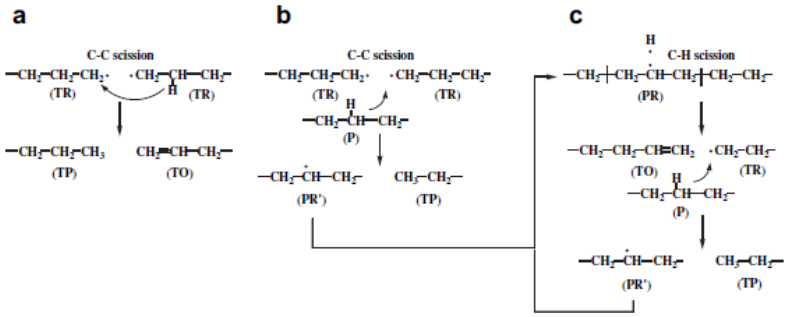

Figure 2.5: Scissioning pathways of main chain: a,b) C-C or c) C-H. The scheme consists of unsaturated (O), saturated (P) or radical (R) scissioning compounds. (T) defines if (O), (P) or (R) is located at the end of the hydrocarbon chain [8].

Similar scissioning mechanism is applied for the PE chain-end scissioning. The *"direct scissioning"* in Figure 2.6 is the dominating pathway and occurs due to the low bonding energy of the carbon placed in the second position of the chain,just as in Figure 2.5 and the C-C pathway (a,b). From this mechanism ethylene is generated. Additional theory about radical propagation transfer and probability of scissioning pathways is presented in the work of Ueno et al. (2010).

Figure 2.6: Primary pathway of end-chain scissioning at temperatures from 590°C, direct scissioning of the terminal group [8].

2.1.2 Composition of primary pyrolysis

Experimental results by Conesa et al. (1994), performed in a Pyroprobe 1000 with high temperatures ($1 - 1400°C$) and fast heating rates ($20°C\ ms^{-1}$), present compositions of the primary pyrolysis of PE. Due to the fast heating rates and small volume of probe, it is assumed by Conesa et al. that only primary pyrolysis of the samples takes place and secondary gas-phase reactions are prevented. According to Table 2.1, the fraction of gaseous compounds in the Pyroprobe increases with the temperature up to 800°C. This can be explained by the conclusions of Seeger and Ritter (Chapter 2.1.1), that scissioning of end-carbon bonds (i.e. volatile compounds) requires more energy and is therefore favored at higher temperatures. A more detailed composition of the gaseous fraction obtained at 800°C is presented in Table 2.2.

Table 2.1: Obtained composition (wt-%) from pyrolysis of HDPE in a Pyroprobe 1000 with nominal heating rate of 20°C ms^{-1}. Residence time of pyrolysis is within milliseconds [14, 15].

Temperature [°C]	**500**	**600**	**700**	**800**	**900**
Gas	2.42	14.62	33.84	37.23	35.82
Waxes	97.58	85.38	66.16	62.77	64.18

Table 2.2: Gas composition (wt-%) from pyrolysis of HDPE in a Pyroprobe 1000 at 800°C. Residence time of pyrolysis is within milliseconds [14, 15].

Methane	1.67	**Propylene**	2.59	**C5**	1.68
Ethane	0.76	**Acetylene**	0.04	**Benzene**	2.34
Ethylene	22.65	**Butylene**	1.58	**Toluene**	0.51
Propane	0.46	**Butane**	2.57	**Xylene**	0.39

The work of Conesa et al. (1994) does not provide detailed information of the remaining composition of waxes. According to Ueno et al. (2010), who could not neglect secondary gas-phase reactions of the scissioning products at high temperatures (800°C), the range of hydrocarbon chains is broad and the carbon numbers evenly distributed. Also, the fraction of olefins exceeds that of paraffins, a trend that increases by temperature, see Table 2.3.

Table 2.3: Composition of gaseous and wax scissioning products (mol-%) obtained from thermal degradation of PE [8].

Temperature [°C]	**590**	**700**	**800**
Diolefin	18	24	21
Olefin	59	61	70
Paraffin	23	15	7

2.2 Formation of aromatic rings

The production of aromatic compounds, in this work referred to as *Tars*, is of great importance for the application of the final product gas. Indeed, if the gas is cooled, the tars will condense and cause damage of equipment or if released to the atmosphere, there is a risk for both health and environmental damage [16]. Already at 500°C, the share of tars is large and the unstable low carbon numbered olefins and paraffins is one of the larger sources of the cyclic compounds [5]. At high temperatures (800°C), 1-ring tar compounds takes part in the formation of more stable 1-ring compounds and polycyclic aromatic hydrocarbons (PAH) [6, 10, 13]. This contributes to the reaction network of the secondary gas-phase reactions being highly complex.

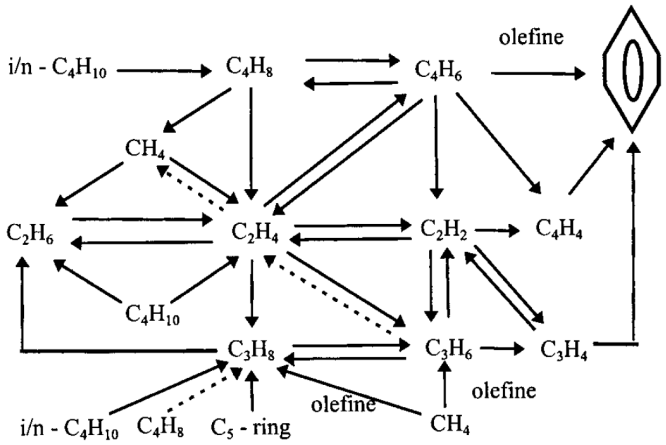

Figure 2.7: Gas-phase reaction scheme of paraffins, olefins and aromatic rings for carbon numbers one to six [10].

2.2.1 1-ring aromatics

According to the proposed reaction scheme of low carbon paraffin, olefin and single aromatic compounds in Figure 2.7, benzene originates from unsaturated and radical compounds of carbon number 3-4. Other literature, treating flame modelling of low carbon olefins, e.g. ethylene, reports 2-, 3- or 4-carbon compounds to be the source of benzene formation [17, 18]. Reaction R1, with recombination of propargyl (C_3H_3) to phenyl (C_6H_5) and thereafter addition of hydrogen to benzene, is presented as the dominating mechanism at atmospheric pressure and high flame temperatures ($\geq 1000K$) [17, 18]. Additionally to R1, benzyne (C_6H_4) as well as reactions between n-C_4H_x and acetylene (C_2H_2), is found to be just as important for the formation of benzene, [17, 18]. It is reported for laminar premixed acetylene and ethylene flames, that R1-R3 achieve maximum reaction rate at 1600, 1000 respectively 700 K [17].

$$\mathrm{C_3H_3^* + C_3H_3^* \rightleftharpoons c\text{-}C_6H_5 + H^* \rightleftharpoons c\text{-}C_6H_6} \tag{R1}$$

$$\mathrm{c\text{-}C_6H_4 + H^* \rightleftharpoons c\text{-}C_6H_6} \tag{R2}$$

$$\mathrm{n\text{-}C_4H_5^* + C_2H_2 \rightleftharpoons c\text{-}C_6H_6 + H^*} \tag{R3}$$

2.2.2 Polycyclic hydrocarbon aromatics

Similar to R1, formation of naphthalene occurs by the combination of two cyclopentadienyl (C_5H_5) according to Reaction R4, which also includes the detachment of two hydrogen radicals [18]. This reaction is presented in the work of Castaldi et al. (1996), and the process is initiated by phenyl oxidation. Other literature, presents the mechanism of hydrogen-abstraction and acetylene-addition (HACA) to describe the formation of PAHs, see Figure 2.8 [19].

$$\text{c-}C_5H_5 + \text{c-}C_5H_5 \rightleftharpoons \text{c-}C_{10}H_8 + H^* + H^* \tag{R4}$$

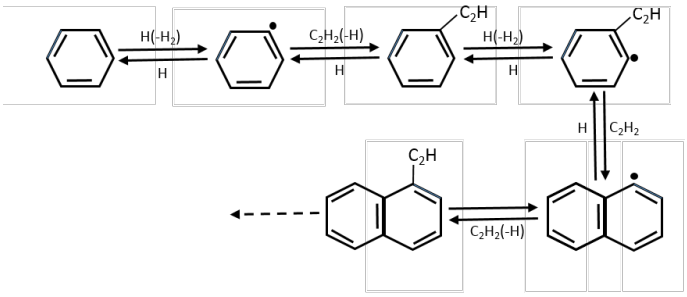

Figure 2.8: Reaction mechanism of hydrogen-abstraction acetylene-addition in the formation of polycyclic hydrocarbon aromatics [19].

2.3 Gasifying agent

In a gasification process, a gasifying agent, e.g. air or steam, is required. During earlier performed experiments of gasification of PE, in the Chalmers gasification unit, steam is used as gasifying agent. For biomass gasification, steam increases heating values and fraction of hydrogen in the produced gas, by the water-gas shift reaction (WGS, Reaction R5), compared to when air or oxygen is used as gasifying agent [20]. Steam has also shown to produce tars that are less refractory and tars that can be more easily reformed by catalytic materials, e.g. benzene and phenols, during gasification of biomass [21].

$$CO + H_2O \rightleftharpoons CO_2 + H_2 \tag{R5}$$

In 1996, Simon et al. conducted research of gasification of polyolefins with steam resulting in high yields of olefins (20-30 wt-% ethylene), similar to processes where naphtha is cracked to olefins (29 wt-% ethylene) in the presence of steam [22]. However, other literature also reports high yield of olefins obtained during pyrolysis of PE, Table 2.2 and 2.3, without the use of steam as gasifying agent [8, 14].

3. Methodology

During this work the process of gasification of polyethylene is examined with the aid of the simulation software ANSYS Chemkin-Pro 18.0 and existing hydrocarbon kinetic mechanisms [23]. The results of simulations are evaluated and discussed in relation to existing experimental data, obtained from the gasification unit in Chalmers Power Central.

3.1 Modelling of the gasification unit

The process steps of gasification of PE, earlier presented in chapter 2.1, are divided into two sub-models according to Figure 3.1 [16]. The focus of this work is the gas-phase reactions occurring after the devolatilization of PE is completed. Similar conditions of temperature, pressure, residence time and steam-fuel ratio applied in the Chalmers gasifier is to be complied in Chemkin. However, the catalytic properties of the bed material used in performed experiments, will be neglected during simulations.

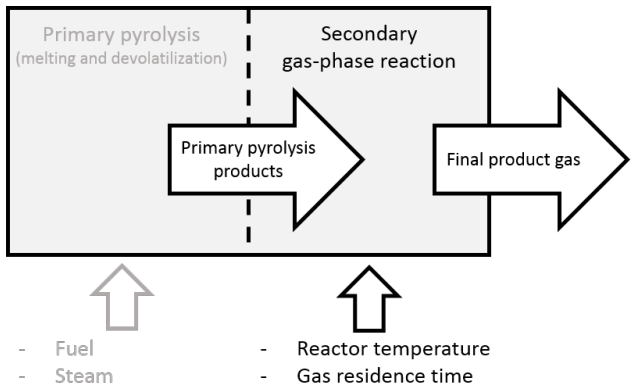

Figure 3.1: The process of gasification of polyethylene divided into sub-models of primary pyrolysis respectively secondary gas-phase reactions.

A schematic of the Chalmers boiler and gasifier system is presented in Figure 3.2. Solid fuel is fed into the gasifier from the top with a purge gas and dropped onto the bed material that consists of Olivine. Heat is provided to the gasifier from the boiler by a dual fluidized bed configuration, meaning bed material is circulated between gasifier and boiler unit.

At the bottom of the gasifier, steam is injected, fluidizing the bed which improves the heat and mass transfer in the reactor. The operating pressure is slightly under atmospheric ($approx. -2kPa$) and within the gasifier temperature is measured continuously at four locations, see overview of the gasifier freeboard and bed in Figure 3.3. As the gas leaves the gasification unit, particles are removed by a heated ceramic filter (T$\geq 350°C$), followed by Solid-Phase Adsoption (SPA) to quantify the tar [24]. The remaining gas flow is cooled and composition of light hydrocarbons and other permanent gases (CO, CO_2 and H_2) is measured with a gas chromatography (GC) system [25].

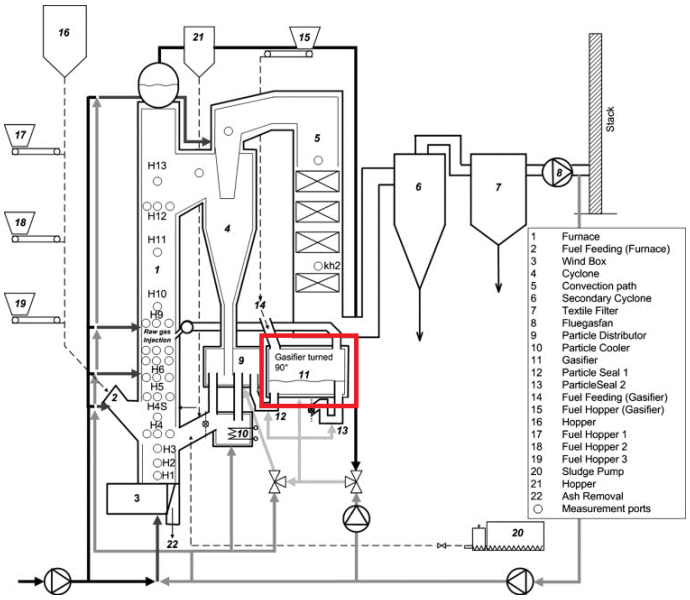

Figure 3.2: Schematic of the combustion-gasification unit in Chalmers Power Central. The gasification unit is marked in red (no. 11) [26].

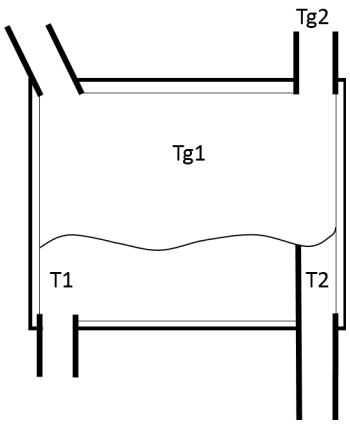

Figure 3.3: Gasifier freeboard and bed. At the bottom bed material is circulated from left to right with two temperature measurements of the bed (T). Fuel input is located at the top left corner and product gas is lead out of the gasifier in the top right corner. Gas temperature (T_g) is measured inside the reactor and at the gas output.

To simulate the model of secondary gas-phase reactions during the gasification of PE presented in Figure 3.1, following assumptions are made:

- Instantaneous and total devolatilization of PE occurs at the bed temperature.
- Primary pyrolysis products is mixed with the injected steam at residence time zero.
- Residence time zero is considered to correspond to just above the bed surface.
- The gaseous compounds moves as a plug flow from the bed surface, through the gasifier freeboard to the exit of the gasifier.
- The catalytic effect of the bed is not considered.
- Rate determining step is the chemical reaction.

With the plug flow model, it is supposed that perfect mixing occurs in the radial direction, but no mixing of species in the axial. The same applies for temperature and pressure. This is a simplification as the fuel is fed in the upper corner of the gasifier. The continuous measurement of in- and output compositions, temperature and pressures in the gasification unit showed almost constant values over time. Therefore, it is considered that the experimental data from the Chalmers gasifier over time corresponds to steady state operation.

3.2 Chemkin modelling

An advantage of ANSYS Chemkin-Pro is the possibility to model gas-phase reactions based on the reaction kinetics schemes. By providing thermodynamic and kinetic data of the reactions considered among the species involved, simulations of the complex reaction mechanisms can be performed. The analysis of simulation results and reaction paths can enhance the understanding of the process and improve design of process, so that the yield of desired products can be maximized.

For this work, thermodynamic and kinetic data is obtained from the CRECK Modeling Group, where a mechanism of 451 species and 17,848 reactions is utilized within the Chemkin-Pro software [23]. The kinetic rate constant (k) is given by two pre-exponential factors (A and β) and the activation energy (E_a), when used in the Arrhenius equation (Eq.1):

$$k(T) = AT^{\beta}e^{\frac{E_a}{RT}} \tag{Eq.1}$$

These parameters originates from both pyrolysis, combustion and partial oxidation processes of hydrocarbon and oxygenated components [23, 27]. No adjustments have been made to the thermodynamic and kinetic files provided by CRECK, with regards to the conditions of this work. Also, the rate determining step for the temperatures considered, is assumed to be the chemical reactions as earlier discussed. Therefore, no data of transport properties is used within these simulations.

The visualization of the model in the Chemkin interface is presented in Figure 3.4, with two separate sources of input, which are mixed without any reactions occurring before entering the plug flow reactor (PFR). It is also determined for the PFR, that Chemkin solves the problem as "Fixed Gas Temperature", which means that the temperature profile for the reactor volume is provided as input to the model.

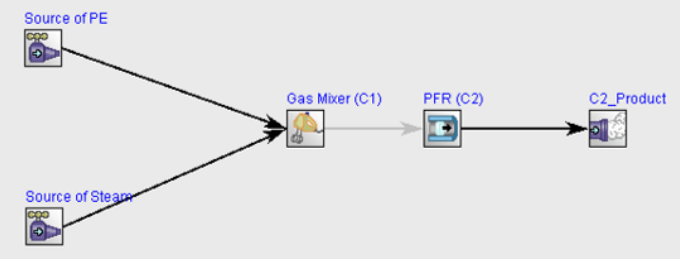

Figure 3.4: Chemkin model of Chalmers Gasifier. From the two *External Sources of Inlet Gas* PE and steam are mixed by a *Non-Reactive Gas Mixer* before entering the *Plug Flow Reactor* (PFR).

The solution of thermodynamics, species, flow properties etc. is retrieved for each step of calculation performed during simulations, and the data can be further processed according to the likes of the user. Additionally, Chemkin possess the alternative of *Reaction Path Analyzer* (RPA), where more detailed information of the reaction mechanisms can be provided. In this work, the reaction pathways related to ethylene, one-ring benzene and two-ring PAH, naphthalene, are studied.

3.2.1 Chemkin input data

The size and inlet temperature of reactant flows, as well as pressure and temperature for the Gas Mixer and PFR is established according to Table 3.1. Inlet temperature at residence time zero, is chosen as the mean of the two experimentally measured bed temperatures T_1 and T_2 (794°C and 787°C) in Figure 3.3. To analyze the influence of the temperature profile, two different profiles was tested during simulations. Temperature profile A, where the inlet temperature is held constant throughout the PFR volume and profile B, with a 100 step linear temperature decrease, from inlet temperature to mean of measured gas temperature, T_{g1} and T_{g2} (748°C and 710°C) in Figure 3.3.

The composition of the PE stream at inlet is considered to consist of *primary pyrolysis products*, with the size and composition of the gas fraction according to earlier published experiments at 800°C in Table 2.1 and 2.2. This temperature is considered reasonable for the assumption of instantaneous and total devolatilization, as the level of temperature profiles used during simulations lies well above that of PE degradation [8, 14].

Table 3.1: Input data of Chemkin model presented in Figure 3.4.

	Temperature [°C]	**Mass flow [g/sec.]**
PE	790	60
Steam	790	71
	Temperature [°C] (input/output)	**Pressure [atm]**
Gas Mixer	790 / 790	1
PFR	790 / 790 (profile A) 790 / 730 (profile B)	1

For the remaining 62.77 wt-% of waxes, different compositions are simulated with hydrocarbon chain-species of high carbon numbers found in the kinetic data obtained from CRECK Modeling Group. Based on the results of Ueno et al. (2010), two compositions of paraffins respectively olefins, are studied for understanding of the effect of the long-chained hydrocarbon, see Table 3.2. The first set includes equal mass fractions of five n-paraffins from carbon number 5-16, and the second set includes four n-olefins of carbon number 5-10.

Table 3.2: Assumed mass fractions of inlet species; paraffins and olefins.

Set	**Compound**	**[wt-%]**
Paraffin	n-C_5H_{12}, n-C_7H_{16}, n-$C_{10}H_{22}$, n-$C_{12}H_{26}$, n-$C_{16}H_{34}$	0.12552
Olefin	n-C_5H_{10}, n-C_6H_{12}, n-C_7H_{14}, n-$C_{10}H_{20}$	0.1569

The dimensions of the PFR, 1x4 meter, is designed to cover a range of residence time (6 s) relevant to the experimental data obtained from the gasification unit at Chalmers.

3.2.2 Chemkin output data

The output compounds from the simulations is selected as the same compounds obtained in the experimental data. Some of the compounds were lumped, as the data files from CRECK only contains one empirical formula for certain compounds, without regards for the isomer, e.g. ortho-/para-xylene or which carbon holding the methyl-group, e.g. 1-/2-naphtol. Also, unknown compounds in the experimental data and compounds not existing in the CRECK data files are discarded. A complete list of the output compounds in Chemkin and the experimental data are found in Table 3.3.

Table 3.3: Complete list of experimental and simulated compounds.

	Experimental	Chemkin
Gas		
	Carbon monoxide	CO
	Carbon dioxide	CO2
	Hydrogen gas	H2
	Steam	H2O
	Oxygen	O2
	Light hydrocarbons	
	Methane	CH4
	Acetylene	C2H2
	Ethylene	C2H4
	Ethane	C2H6
	Propylene	C3H6
	Propane	C3H8
Aromatics/Tars		
	Benzene	C6H6
	Toluene	C7H8
	o-/p-Xylene	XYLENE
	Styrene	C6H5C2H3
	Phenol	C6H5OH
	2,3-benzo(b)furan	BZFUR
	Indene	INDENE
	o-/m-/p-Cresol	CRESOL
	1,2-dihydronaphthalene	C10H10
	Naphthalene	C10H8
	1-/2-methylnaphthalene	C10H7CH3
	Biphenyl	BIPHENYL
	Acenaphthylene	C12H8
	Dibenzofuran	DIBZFUR
	1-/2-naphtol	C10H7OH
	Fluorene	FLUORENE
	Phenanthrene/Anthracene	C14H10
	Pyrene	C16H10

	Discarded species	Empirical formula
	Methyl-styrene 40/60	C9H10
	Acenaphthene	C12H10 (not the same geometry as Biphenyl)
	Xanthene	C13H10O1
	Fluoranthene	C16H10 (not the same geometry as Pyrene)
	Chrysene / Triphenylene	C18H12

3.3 Experimental data

The experimental data provided is obtained from a stable, high temperature (730-790°C, Table 3.1) and low catalytic case; with PE as fuel, steam as gasifying agent (steam to fuel ratio 1.18) and Olivine as bed material. The fuel of PE comes in the form of granules of $D \approx 5$ mm. The values of provided experimental data, are the mean values of continuous measurements over time, of temperatures, pressures and composition of species.

The composition is presented as *mol per kilogram dry, ash-free fuel* for the gaseous light hydrocarbons, respectively *gram per kilogram dry, ash-free fuel* for the tars. As the simulated results of composition is given as concentrations of the wet gas, unit conversion is performed according to Eq.2 and additionally for tars, Eq.3,

$$n_i = \frac{C_i \; u \; A}{\dot{m}_{daf}} \tag{Eq.2}$$

$$m_i = n_i \; M_{w,i} \tag{Eq.3}$$

where n_i denote the moles of each specie $[mol \; {kg_{daf}}^{-1}]$; C_i is the concentration $[mol \; {m^3_{wet}}^{-1}]$; u is the plug flow velocity $[m \; s^{-1}]$; A is the cross section area of the PFR $[m^2]$; $\dot{m}_{daf}$ is the mass flow of dry, ash-free fuel $[kg_{daf} \; s^{-1}]$; m_i is the mass $[gram \; {kg_{daf}}^{-1}]$ and $M_{w,i}$ is the molar weight $[g \; mol^{-1}]$.

4. Results

Simulated results, of the secondary gas-phase reaction sub-model of steam gasification of polyethylene (PE), is presented for the chosen temperature profiles, reactant input compositions and residence time. Product gas output obtained in simulations is compared to existing experimental data. The reaction pathway of significant low carbon olefins and tars is studied with the Chemkin *Reaction Path Analyzer* (RPA).

4.1 Variation of temperature profile, input wax composition and residence time

The assumed sets of primary pyrolysis product composition are tested for both a constant temperature profile (A) and linearly decreasing temperature profile (B). Also, the input of primary pyrolysis products for two different wax compositions is simulated. All simulations is performed over a residence time of 6 seconds and with a steam to fuel ratio of 1.18

4.1.1 Temperature profile

The compositions of light hydrocarbons in the model plug flow, Figure 4.1a, shows that the molar fractions follows the same trends throughout the reactor volume, for both temperature profile A and B. After approximately two seconds of residence time, the formation of light hydrocarbon species starts to slightly deviate between the profiles, e.g. formation of methane (CH_4), as well as the consumption of ethylene (C_2H_4) and propylene (C_3H_6) is slightly higher for the constant temperature profile A, compared to profile B. This agrees with the higher demand of energy for end-group scissioning (chapter 2.1.1), as well as the instability of olefins at high temperature (chapter 2.1).

Regarding the formation of tars, similar effect of the temperature profiles applies. In Figure 4.1b, the constant temperature (A) results in higher yields of tars, compared to when the energy input is reduced over the residence time of the PFR, as in profile B. As the formation of tars is depending on the formation of light hydrocarbons, a delay in formation could have been expected. However, as the the input reactants already includes the degraded products of polyethylene, the formation is instant.

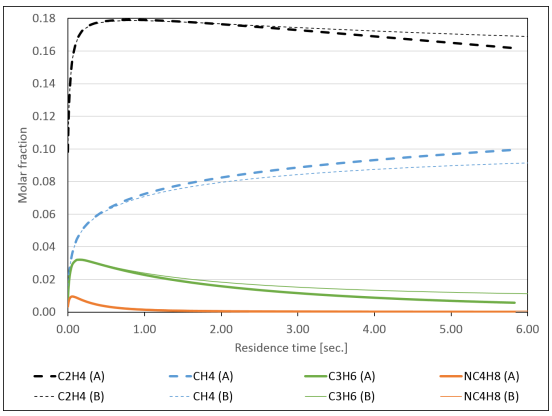

a) Light hydrocarbons

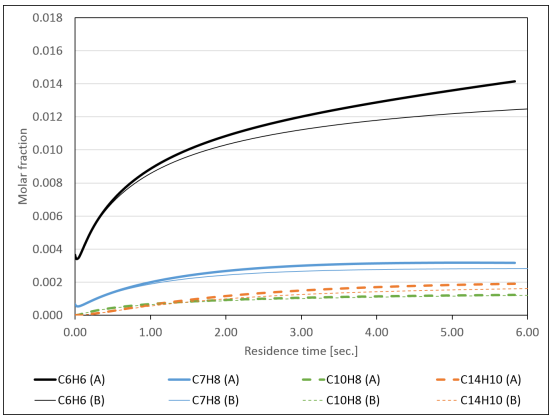

b) Tars

Figure 4.1: Plug flow composition of secondary gas-phase reactions in simulated PFR-model. Residence time 0-6 seconds. Two temperature profiles simulated, A and B (Table 3.1), for input of paraffin-wax (Table 3.2).

For both of the temperature profiles simulated, the progress of plug flow composition is largest during the first second of PFR residence time. Furher on, the compositions of formed light hydrocarbons stays nearly constant throughout the PFR, while the concentrations of tars increases at a faster rate during the first two seconds and thereafter it remains approximately stable. However, the concentration of benzene increases throughout the entire reactor volume.

4.1.2 Input wax composition

The provided sets of input primary pyrolysis products, does not have a considerable impact on the pattern of the plotted specie plug flows, in Figure 4.2a-b. Overall, the input of paraffins results in a higher fraction of ethylene during the first second of residence time, but the composition of light hydrocarbons obtained after the maximum residence time of 6 seconds are similar for both sets of input wax. The formation of tars is different when simulations of the two waxes are compared. Here, the olefin-wax yields higher fraction of tar-compounds throughout the reactor volume.

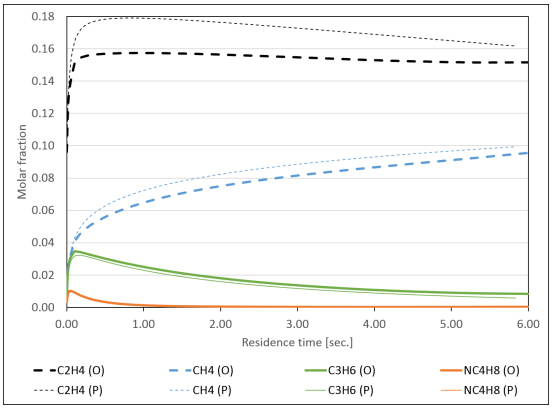

a) Light hydrocarbons

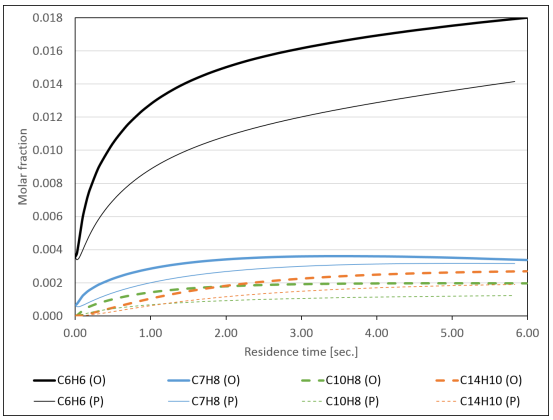

b) Tars

Figure 4.2: Plug flow composition of secondary gas-phase reactions in simulated PFR-model. Residence time 0-6 seconds. Two sets of input wax is simulated (Table 3.2), olefin (O) and paraffin (P), for temperature profile A (Table 3.1).

4.1.3 Residence time

As already mentioned, the yields of molar fractions increases the most at the beginning of the PFR. By examination of the first second of residence time in Figure 4.3a-b, it is detected that the highest molar fraction of ethylene, propylene and butylene is reached within 20 ms. Similarly for the formation of benzene, the highest increase of concentrations is achieved within milliseconds, whereas for the heavier tar-compounds, the maximum yield takes up to three seconds to reach, Figure 4.2b.

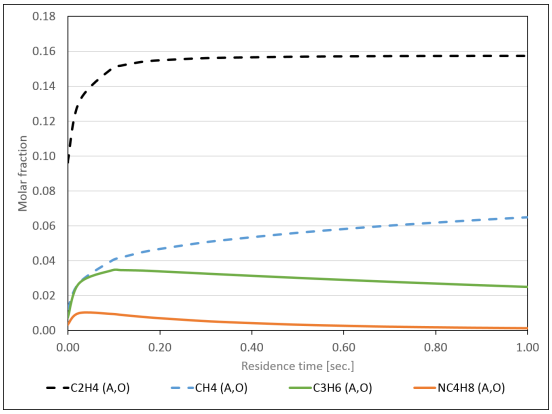

a) Light hydrocarbons

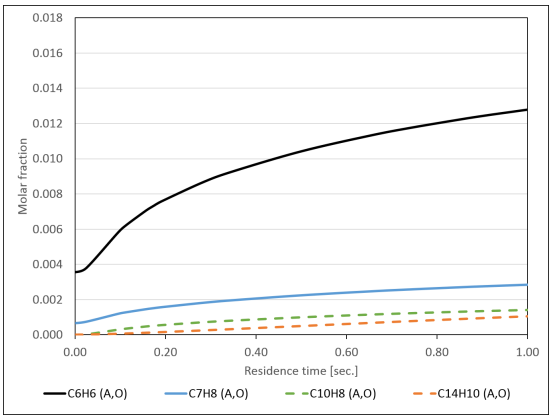

b) Tars

Figure 4.3: Plug flow composition of secondary gas-phase reactions in simulated PFR-model. Input of olefin-wax (Table 3.2) and temperature profile A (Table 3.1). Residence time 0-1 s.

For the simulated results, it is clear that the residence time is of great importance for the ability to control the outlet product composition. If it is desired to obtain high fractions of light hydrocarbons/monomers for polymerization (ethylene) very short residence time (milliseconds) is required for the total process, including both primary pyrolysis and secondary gas-phase reactions. Already after the initial primary pyrolysis of PE, ethylene holds the largest fraction of all compounds formed [14].

4.2 Comparison of model results to experimental data

In literature, earlier studies point out that the fraction of olefins being well above that of paraffin, after the initial primary pyrolysis. Also, as the gasification unit at Chalmers is non-isothermal and the process of PE pyrolysis is endothermic, simulated result of temperature profile B and input of olefin-waxes is chosen for further study and discussion in relation to the experimental data from Chalmers gasification unit.

The experimental data of product composition of cold gas (light hydrocarbons and carbon oxides) and tars, is presented in comparison to simulated results acquired at residence time 0, 2, 4 and 6 seconds, in Figure 4.4 and 4.5.

4.2.1 Cold gas composition

The composition of the cold gas in Figure 4.4, shows quite a large divergence in the distribution of formed compounds, between simulations and experimental results. The rendering of hydrogen gas and carbon oxides are much higher in the gasification unit, compared to the simulated model. The simulated formation of olefins exceed that of the experimental data, while the share of saturated hydrocarbon species is lower in the simulated results.

4.2.2 Tar composition

Opposite to the cold gas composition, the model does obtain similar distribution of the tar compounds in comparison to the experimental data, see Figure 4.5. Benzene, naphthalene, toluene and styrene is holding the largest shares of the displayed tars. However, the simulated yields of some of the heavier PAHs, e.g. Phenanthrene/Anthracene, is not following the same pattern as the experimental data.

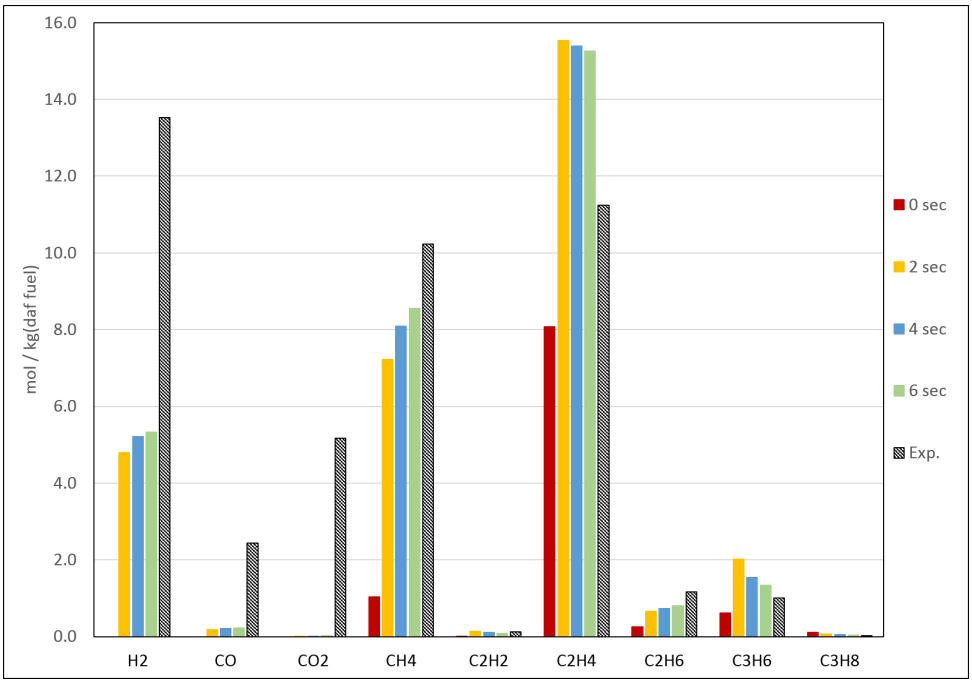

Figure 4.4: Cold gas composition (mol/$kg_{daf fuel}$). Simulated results with set of primary pyrolysis products of equal mass fraction olefins and temperature profile B, for residence time 0, 2, 4 and 6 sec (left to right). Experimental results of stable, high temperature and low activity case with air free, He free and purge gas free product gas (far right).

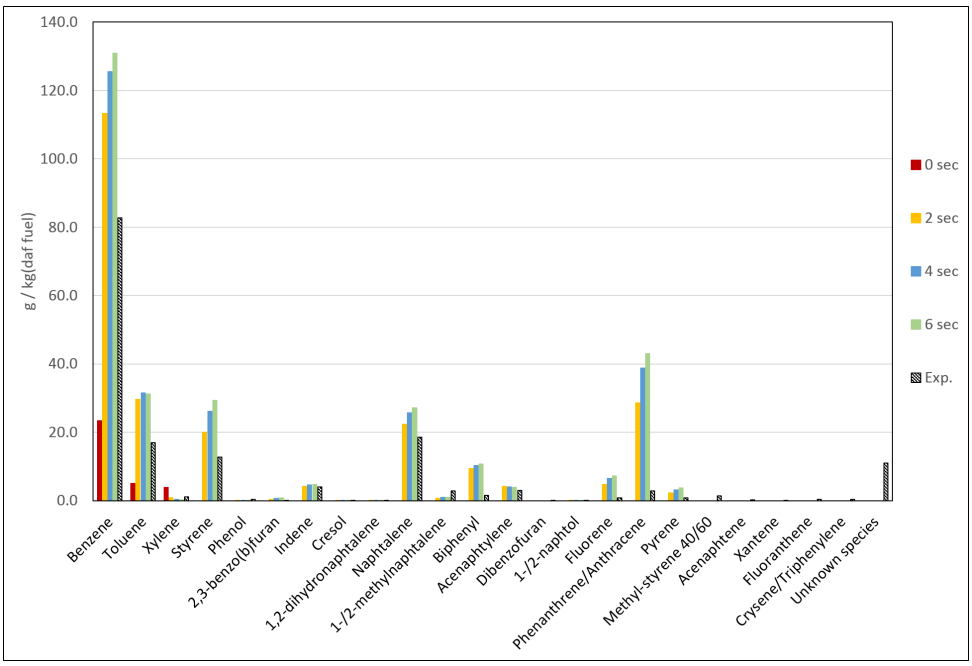

Figure 4.5: Tar composition (g/$kg_{daf fuel}$). Simulated results with set of primary pyrolysis products of equal mass fraction olefins and temperature profile B for residence time 0, 2, 4 and 6 sec (left to right). Experimental results of stable high temperature and low activity case with outlet composition according to Table 3.3 (far right).

4.3 Reaction Network

The simulated results in this work are based on an existing kinetic mechanism of hydrocarbon pyrolysis-, oxidation- and combustion reactions [23]. For the applied model conditions during simulations; constant atmospheric pressure, temperatures of 700-800°C and provided composition of PE primary pyrolysis products, it is of interest to further examine the dominant reactions for some significant low carbon olefins (ethylene, acetylene and propylene), as well as tars (benzene and naphthalene). With the Reaction Path Analyzer (RPA) provided by the Chemkin software, the dominating reactions during simulations of olefin-wax and temperature profile B, is established based on the highest rate of production (ROP). The name of the species given by Chemkin is applied in the chemical reactions presented.

4.3.1 Low carbon olefins

It is already concluded by the simulated results, that the initial formation of ethylene is fast between 0-1 s residence time, and onward the rate of formation/consumption is almost equal, resulting in a constant molar fraction of ethylene (Figure 4.3a). The formation of ethylene start out from Reaction R6, with degradation of a larger hydrocarbon chain to shorter molecules (at 0.0 s):

$$\text{n-}C_6H_{12} \rightarrow 0.25C_2H_4 + 1.5\,C_3H_6 + 0.25\,\text{n-}C_4H_8 \tag{R6}$$

Further on, the dominating reaction for ethylene formation during the first second of PFR residence time, is removal of hydrogen from an ethyl radical:

$$C_2H_5{}^* \rightleftharpoons C_2H_4 + H^* \tag{R7}$$

Mechanism R6-R7 reminds of the work of Ueno et al. (chapter 2.1.1), where long hydrocarbon chains are degraded by radical transfer mechanisms to smaller molecules in repeated sequences, until stable enough configurations is reached. In other, already published literature it is reported, that formation and degradation of ethyl radicals (C_2H_5), Reaction R7, is of great importance in pyrolysis and combustion processes of hydrocarbons, especially in fuel lean processes [28, 29]. Earlier studies also concludes that the reaction has a strong temperature dependence, the formation of ethylene is favoured by high temperatures [28].

As the growth of ethylene is subdued, the continued formation of ethylene now is dominated by degradation of propyl radicals ($C_3H_7^*$) according to Reaction R8.

$$C_3H_7{}^* \rightleftharpoons C_2H_4 + CH_3{}^* \tag{R8}$$

The consumption of ethylene, throughout the PFR, is dominated by the abstraction of hydrogen, Reaction R9, which also is one of the dominating reactions during ethylene combustion processes [28].

$$C_2H_4 + H^* \rightleftharpoons C_2H_3{}^* + H_2 \tag{R9}$$

Acetylene has, according to the HACA-mechanism, an important role in the formation of PAH in combustion processes. In the simulated results of plug flow composition, the quantity of produced of acetylene is insignificant (Figure 4.4) and according to the Chemkin RPA, the ROP for the HACA mechanism is low.

The simulated progress of propylene starts out from the same reaction as ethylene (Reaction R6), before combination of a methyl-allyl radical (SC_4H_7) with an allyl radical (CH_2CHCH_2) or ethylene, is the main source of production.

4.3.2 Tars

The reactions proposed by literature (chapter 2.2, Reaction R1-R4), even though available in the CRECK kinetic data sets, are not to be found within the highest ROP-mechanisms in the simulated results. Initially, the reaction path between either $C_3H_3/C_4H_5/C_2H_2$ and benzene only yields in degradation of benzene into lighter species. Propargyl is instead formed through the reversed Reaction R1. However, after 1 seconds residence time Reaction R1-R3 occurs, but with lower values of ROP compared to the dominating reactions to be presented in this work.

The simulated results with the highest ROP-values, show that benzene initially is formed by reaction of ethylene and pentadiene (C_5H_8) according to Reaction R10. Pentadiene also reacts with benzene to form naphthalene, Reaction R11.

$$C_2H_4 + C_5H_8 \rightarrow \text{c-}C_6H_6 + H_2 + CH_3{}^* + H^* \tag{R10}$$

$$\text{c-}C_6H_6 + C_5H_8 \rightarrow \text{c-}C_{10}H_8 + H_2 + CH_3{}^* + H^*, \tag{R11}$$

The continued progress of benzene formation is through reaction of butyne (C_4H_6) and allyl radicals, followed by combination of cyclic five-carbon and ethylene. Just as in the HACA-mechanism (chapter 2.2.2), benzene is an important specie in the simulated formation of naphthalene. But, according to the simulated results the reaction between benzene and cyclic five-carbon species is the main pathway.

$$\text{c-}C_6H_6 + \text{c-}C_5H_5 \rightarrow \text{c-}C_{10}H_8 + CH_3, \tag{R12}$$

5. Discussion

An assessment of the secondary gas-phase sub-model is further performed, based on the existing experimental data in relation to obtained simulated results and assumptions made for the model. Due to the complexity of the hydrocarbon pyrolysis process, it was appropriate to divide the process into several steps to obtain a more simple model for simulations. Based on published literature, as well as information of earlier conducted experiments at Chalmers Power Central, assumptions and input parameters where established.

5.1 Influence of provided temperature profiles, wax compositions and residence time

Variations of temperature profile provided in simulations performed in this work, do not influence the obtained simulated results to any large extent, as seen in Figure 4.1. The deviation between the two sets of wax compositions is greater in Figure 4.2, were the simulated results with input of olefin-wax did generate lower molar fractions of ethylene and methane, but also higher yields of benzene, naphthalene and phenanthrene, compared to the paraffin-wax. From the obtained simulated results it can be concluded, that for the produced model and provided input data, the choice of temperature profile and wax composition is not of importance.

The most influential parameter of the produced model, is the residence time. The largest progress of the plug flow composition occurs within milliseconds and further, as the plug flow proceeds in time, the concentrations of light hydrocarbons becomes constant, while the fraction of tars increases throughout the entire reactor length. If the object of PE pyrolysis is to obtain short hydrocarbon olefins, the residence time needs to be controlled in order to minimize the formation of unwanted compounds, e.g. tars, during the secondary gas-phase reactions.

5.2 Model results versus experimental data

As expected, the simulated results are not confirmed by the experimental data from Chalmers gasification unit. Overall, the simulated result does show some resemblance to the distribution of hydrocarbon compounds, when compared to existing experimental data. The largest difference between simulations and experimental results, is regarding the distribution of cold gas composition of hydrogen and carbon oxides. A carbon balance over the simulated results, excluded the possibility of calculation errors behind this difference and ensured that the input of carbon matched the output.

Due to the set up of the gasification unit at Chalmers, the experimental data has a distribution of residence times, and the estimate space time has an average of several seconds. The fuel is fed from the top of the unit and pyrolysis of the solid PE-granules is possibly occurring within the entire gasifier freeboard (Figure 3.3). This means that some of the fuel might not reach the bed before pyrolysis starts, which will shortening the residence time. However, the prescribed composition of primary pyrolysis products, i.e. the composition of cold gas and tars at residence time zero in Figure 4.4-4.5, is not either confirming the experimental results.

The assumption of perfectly mixed plug flow is a simplification and more realistic would be to also assume mixing in the axial direction of the plug flow, i.e. mixing species of different "age" of residence time. The current setup of the model, with a perfectly mixed plug flow of compounds of the same age, could perhaps explain why the simulated results obtains higher yields of heavy PAH (e.g. phenanthrene), compared to the experimental results, see Figure 4.5.

If instead the choice of temperature would be lower, the composition of primary pyrolysis products would contain less gaseous compounds and larger share of wax, according to Table 2.1. This could lead to lower simulated yields of light hydrocarbons and tars, more similar to the experimental results in Figure 4.4-4.5. Yet, the differences of produced hydrogen and carbon oxides would be even bigger.

Both the experimental and simulated results has the same steam to fuel ratio, 1.18. The high concentration of steam will overturn the equilibrium of the water-gas shift (WGS) reaction, promoting formation of hydrogen and carbon dioxide. This is also confirmed by examination of the reaction rates in Chemkin. As stated earlier, the catalytic effect of the bed material is neglected in the simulated model. Although the experimental data is obtained from a low catalytic case, the presence of Olivine could explain parts of the higher yields of hydrogen and carbon dioxide, as well as lower yields of heavy PAH in the experimental data compared to simulations. However, the simulated yields of hydrogen is about one third of the experimentally obtained yields, and for the two carbon oxides the differences are greater. The reasoning of Olivine affecting the WGS reaction, forming hydrogen and carbon dioxide, cannot alone explain the difference. Probably, additional steam reforming reactions also contributes to the formation of carbon oxides.

5.3 Secondary gas-phase reaction pathways

When examining the dominating reaction paths in the simulated result, the mechanisms for ethylene shows resemblance to already published literature of PE pyrolysis- and combustion processes. Whereas, the mechanisms with highest rate of production regarding formation of tars are different from the proposed aromatic and PAH formation pathways. The kinetic and thermodynamic data sets used in simulations contains hydrocarbon mechanisms based on processes of both pyrolysis, combustion and partial oxidation [23]. The model conditions or specie concentrations of the simulated results favours the kinetic rate constants of acetylene, benzene and naphthalene mechanisms differently, compared to studied literature of premixed low carbon olefin flames.

5.4 Future questions to be answered

The formulated model produce results with some resemblance to the distribution of hydrocarbon compounds in existing experimental data. However, there are some phenomenons that cannot be explained, based on the work performed. Further, it would be of interest to study the effect of axial mixing on the simulated results. Will mixing of species of different residence time result in lower yields of heavy PAH? Also, specific mechanisms important for the formation of ethylene and tars could be examined explicit, for deeper understanding of how concentrations of species affects the kinetics. How come the proposed mechanisms for benzene and naphthalene is not the dominant reactions within this model? Finally, further development of the sub-model, by including the catalytic effect in the simulated results, could also be a future step forward.

6. Conclusion

In this work, a plug flow model of secondary gas-phase reactions of polyethylene-derived pyrolysis products and steam, is formulated. Based on existing thermodynamic and kinetic data, the model simulates reactions of volatile species, over a residence time of 0-6 seconds. Two temperature profiles and two sets of input reactant composition, are provided in simulations. From the simulated results, it is concluded that the choice of temperature profile and input compositions have low influence on the obtained results. The most influential parameter for the produced model is the residence time, where the largest increase of specie concentrations occurs within 20 ms.

The distribution of simulated hydrocarbon products, show resemblance to that of experimental data obtained from the gasification unit in the Chalmers Power Central, but the yields obtained in simulated results are overestimated for several hydrocarbon species, while the products of water-gas shift reaction are underestimated, compared to the experimental data.

The conditions applied, together with the existing kinetic hydrocarbon mechanism used in simulations, do promote similar reaction pathways related to ethylene, but not regarding the formations of benzene or naphthalene, compared to published literature of polyethylene pyrolysis and combustion processes.

Bibliography

[1] Muralisrinivasan Natamai Subramanian. "Polyethylene". In: *Plastics Waste Management - Processing and Disposal*. Smithers Rapra Technology, 2016, pp. 7–8. ISBN: 978-1-91024-296-4. DOI: 10.1002/0470012668.ch2. URL: https://app.knovel.com/hotlink/khtml/id:kt01129JQ8/plastics-waste-management/references.

[2] Paul T. Williams. "Waste Treatment and Disposal (2nd)". In: John Wiley Sons, Ltd, 2005, pp. 1–49. ISBN: 9780470012666. DOI: 10.1002/0470012668.ch2. URL: http://dx.doi.org/10.1002/0470012668.ch2.

[3] Ellen Macarthur Foundation. *The new Plastics Economy - Rethinking the Future of Plastics*. 2016. URL: https://www.ellenmacarthurfoundation.org/assets/downloads/EllenMacArthurFoundation_TheNewPlasticsEconomy_Pages.pdf.

[4] European Commission. *Communication from the Commission to the European Parliament, the Council, the European Economic and Social Committe and the Committe of the Regions - A European Strategy for Plastics in a Circular Economy*. 2018. URL: http://ec.europa.eu/environment/circular-economy/pdf/plastics-strategy-swd.pdf.

[5] R. W. J. Westerhout et al. "Recycling of Polyethene and Polypropene in a Novel Bench-Scale Rotating Cone Reactor by High-Temperature Pyrolysis". In: *Industrial & Engineering Chemistry Research* 37.6 (1998), pp. 2293–2300. DOI: 10.1021/ie970704q.

[6] J. A. Onwudili, N. Insura, and P. T. Williams. "Composition of products from the pyrolysis of polyethylene and polystyrene in a closed batch reactor: Effects of temperature and residence time". In: *Journal of Analytical and Applied Pyrolysis* 86.2 (2009), pp. 293–303. ISSN: 0165-2370. DOI: 10.1016/j.jaap.2009.07.008. URL: http://www.sciencedirect.com/science/article/pii/S0165237009001119.

[7] H. Hofbauer and V. Wilk. "Conversion of mixed plastic wastes in a dual fluidized bed steam gasifier". In: *Fuel* 107 (2013), pp. 787–799. ISSN: 0016-2361. DOI: https://doi.org/10.1016/j.fuel.2013.01.068. URL: http://www.sciencedirect.com/science/article/pii/S001623611300077X.

[8] Tomonaga Ueno, Erika Nakashima, and Kunihiko Takeda. "Quantitative analysis of random scission and chain-end scission in the thermal degradation of polyethylene". In: *Polymer Degradation and Stability* 95.9 (2010), pp. 1862–1869. ISSN: 0141-3910. DOI: https://doi.org/10.1016/j.polymdegradstab.2010.04.020. URL: http://www.sciencedirect.com/science/article/pii/S0141391010001849.

[9] Merck. *Polyethylene*. 2018. URL: https://www.sigmaaldrich.com/catalog/substance/polyethylene12345900288411?lang=en&region=SE&attrlist=Melting%20Point.

[10] R. W. J. Westerhout, J. A. M. Kuipers, and W. P. M. van Swaaij. "Experimental Determination of the Yield of Pyrolysis Products of Polyethene and Polypropene. Influence of Reaction Conditions". In: *Industrial & Engineering Chemistry Research* 37.3 (1998), pp. 841–847. DOI: 10.1021/ie970384a.

[11] Michael Seeger and Roy J. Gritter. "Thermal Decomposition and Volatilization of Poly($\alpha - olefins$)". In: *Journal of Polymer Science: Polymer Chemistry Edition* 15.6 (1977), pp. 1393–1402. ISSN: 1542-9369. DOI: 10.1002/pol.1977.170150610. URL: http://dx.doi.org/10.1002/pol.1977.170150610.

[12] Katsuhide Murata et al. "Basic study on a continuous flow reactor for thermal degradation of polymers". In: *Journal of Analytical and Applied Pyrolysis* 65.1 (2002), pp. 71–90. ISSN: 0165-2370. DOI: https://doi.org/10.1016/S0165-2370(01)00181-4. URL: http://www.sciencedirect.com/science/article/pii/S0165237001001814.

[13] R Cypres. "Aromatic hydrocarbons formation during coal pyrolysis". In: *Fuel Processing Technology* 15 (1987). Coal Characteristisation for Conversion Processes, pp. 1–15. ISSN: 0378-3820. DOI: https://doi.org/10.1016/0378-3820(87)90030-0. URL: http://www.sciencedirect.com/science/article/pii/0378382087900300.

[14] J. A. Conesa et al. "Pyrolysis of Polyethylene in a Fluidized Bed Reactor". In: *Energy % Fuels* 8.6 (1994), pp. 1238–1246. DOI: 10.1021/ef00048a012. URL: https://doi.org/10.1021/ef00048a012.

[15] A.N. García, R. Font, and A. Marcilla. "Kinetic studies of the primary pyrolysis of municipal solid waste in a Pyroprobe 1000". In: *Journal of Analytical and Applied Pyrolysis* 23.1 (1992), pp. 99–119. ISSN: 0165-2370. DOI: https://doi.org/10.1016/0165-2370(92)80016-F. URL: http://www.sciencedirect.com/science/article/pii/016523709280016F.

[16] D. Fuentes-Cano et al. "Kinetic Modeling of Tar and Light Hydrocarbons during the Thermal Conversion of Biomass". In: *Energy Fuels* 30.1 (2016), pp. 377–385. ISSN: 0887-0624. DOI: 10.1021/acs.energyfuels.5b02131.

[17] Hai Wang and Michael Frenklach. "A detailed kinetic modeling study of aromatics formation in laminar premixed acetylene and ethylene flames". In: *Combustion and Flame* 110.1 (1997), pp. 173–221. ISSN: 0010-2180. DOI: https://doi.org/10.1016/S0010-2180(97)00068-0. URL: http://www.sciencedirect.com/science/article/pii/S0010218097000680.

[18] Marco J. Castaldi et al. "Experimental and modeling investigation of aromatic and polycyclic aromatic hydrocarbon formation in a premixed ethylene flame". In: *Symposium (International) on Combustion* 26.1 (1996), pp. 693–702. ISSN: 0082-0784. DOI: https://doi.org/10.1016/S0082-0784(96)80277-3. URL: http://www.sciencedirect.com/science/article/pii/S0082078496802773.

[19] Hai Wang and Michael Frenklach. "Calculations of Rate Coefficients for the Chemically Activated Reactions of Acetylene with Vinulic and Aromatic Radicals". In: *The Journal of Physical Chemistry* 98.44 (1994), pp. 11465–11489.

DOI: 10.1021/j100095a033. URL: https://pubs-acs-org.proxy.lib.chalmers.se/doi/abs/10.1021/j100095a033.

[20] A. Gómez-Barea and B. Leckner. "Modeling of biomass gasification in fluidized bed". In: *Progress in Energy & Combustion Science* 36.4 (2010), pp. 444–509. DOI: 10.1016/J.PECS.2009.12.002.

[21] A. Milne, N. Abatzaglou, and Robert Evans. "Biomass Gasifier "Tars": Their Nature, Formation, and Conversion". In: (Jan. 1998).

[22] C.M. Simon, W. Kaminsky, and B. Schlesselmann. "Pyrolysis of polyolefins with steam to yield olefins". In: *Journal of Analytical and Applied Pyrolysis* 38.1 (1996), pp. 75–87. ISSN: 0165-2370. DOI: https://doi.org/10.1016/S0165-2370(96)00950-3. URL: http://www.sciencedirect.com/science/article/pii/S0165237096009503.

[23] CRECK Modeling Group. *Kinetic Mechanisms, Complete Mechanism (Version 1412, December 2014)*. 2018. URL: http://creckmodeling.chem.polimi.it/.

[24] Mikael Israelsson, Martin Seemann, and Henrik Thunman. "Assessment of the Solid-Phase Adsorption Method for Sampling Biomass-Derived Tar in Industrial Environments". In: *Energy & Fuels* 27.12 (2013), pp. 7569–7578. DOI: 10.1021/ef401893j. URL: https://doi.org/10.1021/ef401893j.

[25] Anton Larsson et al. "Evaluation of Performance of Industrial-Scale Dual Fluidized Bed Gasifiers Using the Chalmers 24-MWth Gasifier". In: *Energy & Fuels* 27.11 (2013), pp. 6665–6680. DOI: 10.1021/ef400981j. URL: dx.doi.org/10.1021/ef400981j.

[26] H. Thunman et al. "Using an oxygen-carrier as bed material for combustion of biomass in a 12-MWth circulating fluidized-bed boiler". In: *Fuel* 113 (2013), pp. 300–309. ISSN: 0016-2361. DOI: https://doi.org/10.1016/j.fuel.2013.05.073. URL: http://www.sciencedirect.com/science/article/pii/S0016236113004857.

[27] E. Ranzi et al. "Hierarchical and comparative kinetic modeling of laminar flame speeds of hydrocarbon and oxygenated fuels". In: *Progress in Energy and Combustion Science* 38.4 (2012), pp. 468–501. ISSN: 0360-1285. DOI: https://doi.org/10.1016/j.pecs.2012.03.004. URL: https://www.sciencedirect.com/science/article/pii/S0360128512000196?via%5C%3Dihub.

[28] Henning Richter and Jack B. Howard. "Formation and consumption of single-ring aromatic hydrocarbons and their precursors in premixed acetylene, ethylene and benzene flames". In: *Phys. Chem. Chem. Phys.",* 4.11 (2002), pp. 2038–2055. DOI: 10.1039/B110089K. URL: http://dx.doi.org/10.1039/B110089K.

[29] Phillip D. Lightfoot and Michael J. Pilling. "Temperature and pressure dependence of the rate constant for the additon of hydrogen atoms to ethylene". In: *The Journal of Physical Chemistry* 91.12 (1987), pp. 3373–3379. DOI: 10.1021/j100296a054. URL: https://pubs.acs.org/doi/abs/10.1021/j100296a054.